

Two-Stage Plans for Estimating a Threshold Value of a Regression Function

RUNLONG TANG¹, MOULINATH BANERJEE², GEORGE MICHAILIDIS², AND SHAWN MANKAD²

¹*Department of Operations Research and Financial Engineering, Princeton University*

²*Department of Statistics, University of Michigan*

Abstract

This study investigates two-stage plans based on nonparametric procedures for estimating an inverse regression function at a given point. Specifically, isotonic regression is used at stage one to obtain an initial estimate followed by another round of isotonic regression in the vicinity of this estimate at stage two. It is shown that such two stage plans accelerate the convergence rate of one-stage procedures and are superior to existing two-stage procedures that use local parametric approximations at stage two when the available budget is moderate and/or the regression function is ‘ill-behaved’. Both Wald and Likelihood Ratio type confidence intervals for the threshold value of interest are investigated and the latter are recommended in applications due to their simplicity and robustness. The developed plans are illustrated through a comprehensive simulation study and an application to car fuel efficiency data.

1. INTRODUCTION

Threshold estimation is a canonical statistical estimation problem with numerous applications in science and engineering. Here is an interesting motivating example. In recent years, an important consideration for both car manufacturers and potential buyers in the United States is the fuel efficiency of the vehicle, expressed in miles per gallon (MPG). The National Highway Traffic Safety

Administration (NHTSA) regulates the Corporate Average Fuel Economy (CAFE) standards to encourage automobile manufacturers to improve the average fuel efficiency of their fleets of vehicles. The CAFE standard for 2012 models is 29.8 MPG, set to increase to 34.3 MPG in 2016 according to the Environmental Protection Agency rule that came into effect in August 2012. To encourage higher fuel efficiency, manufacturers are subject to a penalty if the average FE of their fleets falls below the CAFE standard. Moreover, a so-called gas guzzler tax is imposed on cars with low FE in accordance with the US Energy Tax Act of 1978.

The data on fuel efficiency as a function of the vehicle's horse power, which is a key component, for the 2012 models is shown in Figure 1 (for a detailed discussion of the data and CAFE standards, see section 4). An expected decreasing relationship is observed and it is of interest to identify the horse power threshold at which the fuel efficiency meets the current CAFE, as well as the 2016 standard.

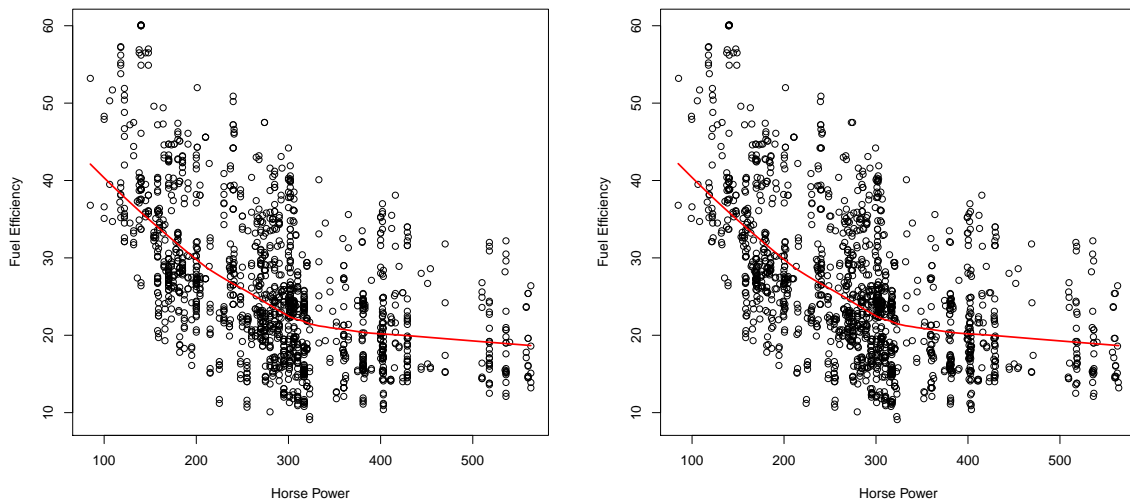


Figure 1: Scatterplots of the relationship between horse power and fuel efficiency of naturally aspirated vehicles; $FE = m(HP)$. The right panel shows the data with jittered horsepower to create a unique horsepower for every observation.

The data plot indicates that fitting a precise parametric model may be challenging, while it

is rather straightforward to fit a monotonically decreasing nonparametric one and obtain the fuel efficiency threshold for the target values of ~ 30 and ~ 34 . However, it is also desirable to assign a confidence interval around the estimate and an interesting question addressed in this paper is whether an *adaptive procedure* can lead to improved precision for such threshold estimates.

The topic of using adaptive procedures in a *design setting* for threshold estimation models has been recently studied in the literature (Lan et al., 2009; Tang et al., 2011). The basic model considered is $Y = m(X) + \epsilon$, where the design point X takes values in $[a, b]$, the regression function m is monotone, for the sake of presentation henceforth assumed non-decreasing, and the random error ϵ has mean 0 and finite variance σ^2 . The quantity to be estimated is a threshold d_0 , which in (Lan et al., 2009) corresponded to a change-point (i.e. $m(X) = \alpha_0 1(x \leq d_0) + \beta_0 1(x > d_0)$ with unknown constants α_0 and β_0), whereas in Tang et al. (2011) to $d_0 = m^{-1}(\theta_0)$ for some prespecified θ_0 .

The employed two-stage adaptive procedure in Lan et al. (2009) and Tang et al. (2011) works as follows: (i) in the first stage, it utilizes a portion p of the design budget to obtain an initial estimate of d_0 , (ii) in the second stage, the remaining portion $(1 - p)$ of the budget is used to obtain more sample points in a small neighborhood of that estimate; (iii) finally, an improved estimate based on the second-stage data is constructed. This more intense “zoom-in” sampling leads to *accelerated* convergence rates of the second stage estimators for d_0 compared to the standard ones that use all the data in one shot. Specifically, for the change point problem, the rate can be accelerated from n to almost n^2 (up to a logarithmic factor) as in (Lan et al., 2009), while for the inverse regression problem, from $n^{1/3}$ to $n^{1/2}$ by employing a local linear approximation (Tang et al., 2011), where n denotes the total budget available. Hence, tighter confidence intervals can be constructed that have the correct nominal coverage with the same budget as standard one-stage procedures, or alternatively one can reduce the design budget and still have good quality confidence intervals.

In this paper, given our motivating data application, we focus on the second problem, namely that of estimating the inverse regression function at a prespecified point θ_0 . This is closely related to dose response (Rosenberger and Haines, 2002) and statistical calibration studies (Osborne, 1991)

(for additional references see [Tang et al. \(2011\)](#)). As mentioned above, a strategy that obtains a first stage estimate using isotonic regression, followed by a local linear approximation, gives a consistent second stage estimator that achieves the parametric rate \sqrt{n} . However, the success of this strategy *heavily hinges upon the (approximate) linearity of the regression function $m(\cdot)$ in the vicinity of d_0* . Small departures from linearity do not adversely affect the results (especially when the budget is large enough to allow for significant “zooming-in” at the second stage), but severe departures are a totally different matter as illustrated next.

Consider a monotone regression function exhibiting strong nonlinearity at $d_0 = 0.5$, for example, given by $m(x) = (1/40)\sin(6\pi x) + 1/4 + (1/2)x + (1/4)x^2$ with $x \in [0, 1]$ (see the left panel of Figure 4 for its plot). The coverage rates and average lengths of the confidence intervals obtained from the two-stage adaptive strategy based on isotonic regression and a local linear approximation for selected total budget sizes ($n = 100, 300, 500$), varying portions p allocated to the first stage and different noise levels ($\sigma = 0.1, 0.3, 0.5$) are depicted in Figure 2.

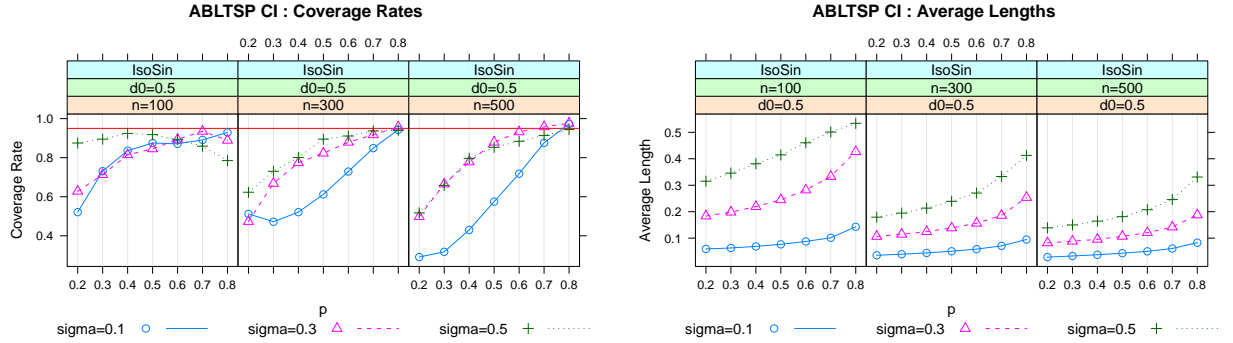


Figure 2: The left panel shows the coverage rates of the 95% confidence intervals using a local linear approximation for $d_0 = 0.5$ with different sample sizes, and noise levels. The right panel shows the corresponding average lengths of the intervals.

It can be seen that for the majority of portions p , the confidence intervals constructed from this adaptive strategy fail miserably in terms of coverage rates and exhibit relatively large lengths. Of interest is the fact that for large p , the coverage rates indeed approach the nominal level. In

practice, however, it is not possible to choose an appropriate p without prior information on m . Further, even for large p 's, the confidence intervals are excessively wide, especially for large noise levels.

In contrast, a two stage adaptive strategy based on employing isotonic regression at both stages, which will be fully developed in this paper, overcomes these difficulties. Such a strategy would be also desirable for the motivating data application, due to high variability in the vicinity of the CAFE thresholds, as seen in the scatterplots of Figure 1. In Figure 3, the coverage rates and average lengths using our new strategy are shown for the same settings as above, but with $p = 1/4$ (for more on this universal choice of p see Section 2). It can be seen that this wholly nonparametric strategy overcomes the previous difficulties, proves robust to the level of local nonlinearity of the regression function m and, as argued in Section 2, is easy to implement.

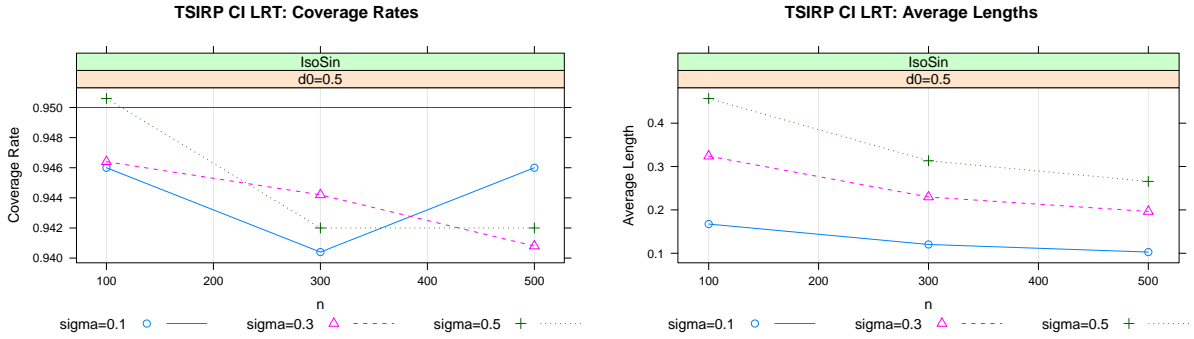


Figure 3: The left panel shows the coverage rates of the 95% confidence intervals using a two stage procedure for $d_0 = 0.5$ with different sample sizes, and noise levels. The right panel shows the corresponding average lengths of the intervals.

The remainder of the paper is organized as follows: in Section 2 the adaptive procedure is introduced and the main results presented. Section 3 presents extensive simulations results, while an interesting application of the methodology to fuel efficiency data is shown in Section 4. Section 5 concludes. Proofs are sketched in the appendix.

2. TWO STAGE ADAPTIVE PROCEDURES

2.1 An Overview of the Isotonic Regression Procedure

We provide a brief description of the one-stage isotonic regression procedure (OSIRP). Specifically, given n fixed or random design points $\{X_i\}_{i=1}^n$ in $[a, b]$ distributed according to a continuous design density g and the corresponding responses $\{Y_i\}_{i=1}^n$, obtained from the proposed model, the isotonic regression estimate of $m(\cdot)$ is given by

$$m_I(x) = m_1^* 1\{x \in [a, X_1]\} + \sum_{i=1}^{n-1} m_i^* 1\{x \in [X_i, X_{i+1})\} + m_n^* 1\{x \in [X_n, b]\} \quad (2.1)$$

where $\{m_i^*\}_{i=1}^n = \underset{m_1 \leq m_2 \leq \dots \leq m_n}{\text{Argmin}} \sum_{i=1}^n (Y_i - m_i)^2$. This minimizer exists uniquely, has a nice geometric characterization as the slope of the greatest convex minorant of a stochastic process and is readily computable using the pool adjacent violators algorithm (PAVA) (see, for example, Robertson et al. (1988)). Then, for a prespecified value $\theta_0 \in (m(a), m(b))$, the one-stage isotonic regression estimator of d_0 is defined by

$$d_I = m_I^{-1}(\theta_0) = \inf\{x \in [a, b] : m_I(x) \geq \theta_0\}, \quad (2.2)$$

where $\inf\{\emptyset\} = b$. Under mild conditions on the regression function and the design density, namely

Assumption A: m is once continuously differentiable in a neighborhood of d_0 with positive derivative $m'(d_0)$ and g is positive and continuous at d_0 ,

the asymptotic distribution of d_I is given by (see [Tang et al. \(2011\)](#)):

$$n^{1/3}(d_I - d_0) \xrightarrow{d} C_{d_I} g(d_0)^{-1/3} \mathcal{Z}, \quad (2.3)$$

where $C_{d_I} = (4\sigma^2/m'(d_0)^2)^{1/3}$ and \mathcal{Z} follows the standard Chernoff distribution ([Groeneboom and Wellner \(2001\)](#)). This result can be used to construct a $1 - \alpha$ Wald-type confidence interval for d_0 :

$$\left[d_I \pm n^{-1/3} \widehat{C_{d_I}} \widehat{g(d_0)}^{-1/3} q(\mathcal{Z}, 1 - \alpha/2) \right],$$

where the hats denote consistent estimates and $q(\xi, \tau)$ is the lower τ 'th quantile of a random variable ξ .

An alternative is to construct confidence intervals through likelihood ratio (LR) testing. Specifically, the hypotheses of interest are

$$H_0 : m^{-1}(\theta_0) = d_0 \leftrightarrow H_a : m^{-1}(\theta_0) \neq d_0. \quad (2.4)$$

Then, the LR test statistic is given by

$$2 \log \lambda_I = 2 \log \lambda_I(d_0) = 2 [l_n(m_I, \hat{\sigma}) - l_n(m_{Ic}, \hat{\sigma})], \quad (2.5)$$

where $l_n(m, \sigma) = -(2\sigma^2)^{-1} \sum_{i=1}^n (Y_i - m(X_i))^2$, m_{Ic} is the constrained isotonic regression of m under H_0 and $\hat{\sigma}$ a consistent estimate of σ . It is known that m_{Ic} uniquely exists (see [Banerjee \(2000\)](#)). The asymptotic distribution of $2 \log \lambda_I$ under H_0 is given in ([Banerjee, 2009](#)): $2 \log \lambda_I \xrightarrow{d} \mathbb{D}$, where \mathbb{D} is a ‘universal’ random variable not depending on the parameters of the model ([Banerjee and Wellner \(2001\)](#)). This result allows us to construct a $1 - \alpha$ LR-type confidence region for d_0 :

$$\{x \in [a, b] : 2 \log \lambda_I(x) \leq q(\mathbb{D}, 1 - \alpha)\}. \quad (2.6)$$

The LR-type confidence region can be shown to be an interval and is typically *asymmetric* around d_I , unlike the Wald-type one. Its main advantage is that only σ needs to be estimated for its construction, whereas for the Wald confidence interval, estimation of $m'(d_0)$ is also needed, a significantly more involved task.

Remark 2.1. The use of the term LR statistic in connection with 2.5 needs to be clarified. Under a normality assumption on the errors, $2 \log \lambda_I$ is, indeed, a proper likelihood ratio statistic; otherwise, it is more accurately a *residual sum of squares statistic* which can be interpreted as a ‘working likelihood ratio statistic’ where the normal likelihood is used as a working likelihood. In this paper, we do not assume normality of errors but continue to use the term LR statistic for $2 \log \lambda_I$ in the above sense.

2.2 Adaptive Two-Stage Procedures

As noted in Introduction, adaptive two stage procedures can lead to accelerated convergence rates and hence to sharper confidence intervals for d_0 . The main steps of such a two-stage fully nonparametric procedure are outlined next:

1. Denote by $p \in (0, 1)$ the sample proportion to be allocated in the first stage and by $n_1 = \lfloor np \rfloor$ and $n_2 = n - n_1$, the corresponding first and second stage sample sizes, respectively.
2. Generate the first stage data $\{(X_{1,i}, Y_{1,i})\}_{i=1}^{n_1}$ with a design density g_1 on $[a, b]$. Then, compute a first stage monotone non-parametric estimator \hat{m}_1 of m and obtain the corresponding first stage estimator $d_{1,I} = \hat{m}_1^{-1}(\theta_0)$ of d_0 for a prespecified value θ_0 .
3. Specify the second stage sampling interval $[L_1, U_1] = [d_{1,I} \pm C_1 n_1^{-\gamma_1}] \cap [a, b]$ where $C_1 > 0$ and $0 < \gamma_1 < \gamma^* < 1/2$, γ^* being the convergence rate of \hat{d}_1 .
4. Obtain the second stage data $\{(X_{2,i}, Y_{2,i})\}_{i=1}^{n_2}$ with a design density g_2 on $[L_1, U_1]$. Employ these data and a non-parametric procedure (which could be different from the one used previously) to compute a monotone second stage estimator $m_{2,I}$ and, as in the first stage, the corresponding $d_{2,I}$.
5. Construct confidence intervals for d_0 using the asymptotic distribution of $d_{2,I}$.

Remark 2.2. Choosing $\gamma_1 < \gamma^*$ ensures that the stage two sampling interval contains d_0 with probability going to 1.

2.3 Asymptotic Properties of Two-Stage Estimators

We discuss the properties of the two-stage procedure, where isotonic regression is employed in both stages (henceforth, IR+IR).

Proposition 1. *Consider the IR + IR procedure. Let the design density at stage two be given by: $g_2(x) = (C_1 n_1^{-\gamma_1})^{-1} \psi((x - d_{1,I})/C_1 n_1^{-\gamma_1})$ where ψ is a Lebesgue density on $[-1, 1]$ that is positive at 0 and continuous in a neighborhood of 0. Thus, g_2 is simply ψ renormalized to the sampling interval at stage two. Assume that m' , the derivative of m , exists and is continuous in a neighborhood of d_0 and $m'(d_0) > 0$. Let $d_{2,I} = m_{2,I}^{-1}(\theta_0)$ where $m_{2,I}$ is the isotonic estimator of m constructed from the second stage data. Then, $n^{(1+\gamma_1)/3}(d_{2,I} - d_0) \xrightarrow{d} C_{d_{2,I}} \mathcal{Z}$, where $C_{d_{2,I}} = C_{d_I} \left(\frac{C_1}{(1-p)p^{\gamma_1}\psi(0)} \right)^{1/3}$.*

From Proposition 1, a Wald-type $1 - \alpha$ asymptotic confidence interval for d_0 is given by

$$[d_{2,I} \pm n^{-(1+\gamma_1)/3} \widehat{C_{d_{2,I}}} q(\mathcal{Z}, 1 - \alpha/2)]. \quad (2.7)$$

Remark 2.3. A consequence of the accelerated rate of convergence obtained with the IR+IR strategy is that the asymptotic relative efficiency (ARE) of the two-stage estimator $d_{2,I}$ with respect to the one-stage estimator d_I is

$$ARE(d_{2,I}, d_I) = \frac{s.d.(d_I)}{s.d.(d_{2,I})} = \left(\frac{(1-p)p^{\gamma_1}\psi(0)}{C_{1g}(d_0)} \right)^{1/3} n^{\gamma_1/3} \rightarrow \infty \text{ as } n \rightarrow \infty.$$

Note that, in the generic description of the two-stage procedure above, we use a confidence interval for d_0 that relies on the asymptotic distribution of a point estimate computed at stage two. However, this is not the only way to proceed at stage two. Having collected the second stage data at the beginning of Step 4, we can bypass point estimation altogether and construct a confidence interval using likelihood ratio inversion. This alternative possibility is discussed below. Also, as will be explained in the practical implementation, the construction of $[L_1, U_1]$ is achieved in practice by constructing a high probability confidence interval for d_0 from the stage one data. This also opens up the possibility of bypassing point estimates at stage one in favor of a likelihood ratio inversion based confidence interval, a point that we come to later.

An alternative LR-type CI can be constructed as follows: the LR-type test statistic at stage two for testing $H_0 : d_0 = m^{-1}(\theta_0)$ is

$$2 \log \lambda_{2,I} = 2 \log \lambda_{2,I}(d_0) = 2 [l_n(m_{2,I}, \hat{\sigma}) - l_n(m_{2,Ic}, \hat{\sigma})], \quad (2.8)$$

where $l_n(m, \sigma) = -\frac{1}{2\sigma^2} \sum_{i=1}^{n_2} (Y_{2,i} - m(X_{2,i}))^2$, $m_{2,Ic}$ is the constrained estimator of m under the null hypothesis H_0 and $\hat{\sigma}$ is a consistent estimate of σ .

Proposition 2. *Under the assumptions of Proposition 1, and the null hypothesis $H_0: m^{-1}(\theta_0) = d_0$ holding true, we have $2 \log \lambda_{2,I} \xrightarrow{d} \mathbb{D}$, where \mathbb{D} is as before.*

Finally, from Proposition 2, an LR-type $(1 - \alpha)$ asymptotic confidence interval for d_0 is given by

$$\{x \in [a, b] : 2 \log \lambda_{2,I}(x) \leq q(\mathbb{D}, 1 - \alpha)\}. \quad (2.9)$$

For the theoretical derivations in connection with Propositions 1 and 2, see the Appendix.

Remark 2.4. We have focused on the case of two-stage adaptive designs and the acceleration of the convergence rate by an IR+IR strategy. Obviously, one can extend it to multiple stages and continue using isotonic regression. As outlined in Section S1 in the Supplement, it can be established that the convergence rate of such a procedure would come *arbitrarily close* to the \sqrt{n} parametric rate, if enough stages are employed, *but would not achieve it*.

2.4 Implementation Issues

We discuss, next, the main steps for implementing the IR+IR strategy in practice. Specifically, we address the following: (i) estimation of σ^2 , (ii) estimation of m' , (iii) determination of second stage sampling interval $[L_1, U_1]$, (iv) the first stage sampling proportion p .

Implementation of IR + IR: For the estimation of σ^2 at Stage 1, we employ the nonparametric estimator proposed by Gasser et al. (1986), and for the estimation of $m'(d_0)$, the local quadratic regression procedure proposed by Fan and Gijbels (1996); some details are provided in Section 3. Next comes the determination of the second stage sampling interval. Recall, that the theoretical formula for the interval is given by $[d_{1,I} \pm C_1 n_1^{-\gamma_1}]$, with $C_1 > 0$ and $\gamma_1 \in (0, 1/3)$. While any such interval will contain d_0 with probability going to 1 in the long run, in practice we would like to ensure that our prescribed sampling interval $[L_1, U_1]$ does trap d_0 with high probability. The practical determination of $[L_1, U_1]$ is therefore achieved through a high probability confidence interval for d_0 from Stage 1 data. Consider the the following $1 - \beta$ Wald-type confidence interval

$$[d_{1,I} \pm n_1^{-1/3} \hat{C}_{d_I} g_1(d_{1,I})^{-1/3} q(\mathcal{Z}, 1 - \beta/2)] \cap [a, b], \quad (2.10)$$

where the computation of \hat{C}_{d_I} involves estimating both σ^2 and $m'(d_0)$ and where β is a small positive number such as 0.01. Using this, in practice, as $[L_1, U_1]$ amounts to choosing C_1 and γ_1 such that

$C_1 n_1^{-\gamma_1} = n_1^{-1/3} \hat{C}_{d_I} g_1(d_{1,I})^{-1/3} q(\mathcal{Z}, 1 - \beta/2)$. That is, $\gamma_1 = 1/3$ and $C_1 = \hat{C}_{d_I} g_1(d_{1,I})^{-1/3} q(\mathcal{Z}, 1 - \beta/2)$. Although $\gamma_1 = 1/3$ is not in $(0, 1/3)$ as required by our theoretical results, it nevertheless provides a good approximation in practice, since it lies at the boundary of that interval.

As far as the first stage sampling proportion is concerned, one would like to choose this in such a way as to increase the precision of the second stage isotonic estimator. Proposition 1 shows that the second stage estimator is asymptotically unbiased and that its standard deviation is proportional to $\{(1 - p)p^{\gamma_1}\}^{-1/3}$. For a fixed γ_1 , this is minimized when $\log(1 - p) + \gamma_1 \log p$ is maximized, which happens when $p = p_{opt} = \gamma_1/(1 + \gamma_1)$. As γ_1 approaches $1/3$, p_{opt} approaches $1/4$. Thus, the optimal practical allocation of budget at Stage 1 is 25%.

From Stage 2 data, we can construct a confidence interval for d_0 based on $d_{2,I}$ following Proposition 1 in which case both $m'(d_0)$ and σ^2 need to be updated. Alternatively, we can use likelihood ratio inversion to get a CI of desired coverage for d_0 , following Proposition 2 in which case only the estimate of σ^2 needs to be updated. Finally, a third option is to bypass the estimation of $m'(d_0)$ altogether by prescribing a high probability LR based confidence interval for d_0 as $[L_1, U_1]$ in Stage 1 and then using LR inversion at Stage 2 as well. While this procedure does not quite fall within the purview of our theoretical results it is a natural methodological choice; furthermore, comparisons among these three approaches based on elaborate simulation studies demonstrate that it is superior to the other two in practice.

3. PERFORMANCE EVALUATION OF THE ADAPTIVE PROCEDURES

In this study, the following procedures are compared: (i) practical one-stage procedure based on isotonic regression (POSIRP) with Wald and LR CIs, (ii) practical two-stage procedure based on isotonic regression (PTSIRP-Wald) for both stages and using Wald CIs both for selecting (L_1, U_1) and constructing the final CI, (iii) practical two-stage procedure (PTSIRP-LR) similar to (ii) but employing LR CIs in both stages and (iv) the procedure from Tang et al. (2011) that uses isotonic regression followed by a local linear approximation and bootstrapping for constructing CIs for d_0 (PABLTSP). The use of the qualifier ‘Practical’ before the various procedures above is to emphasize

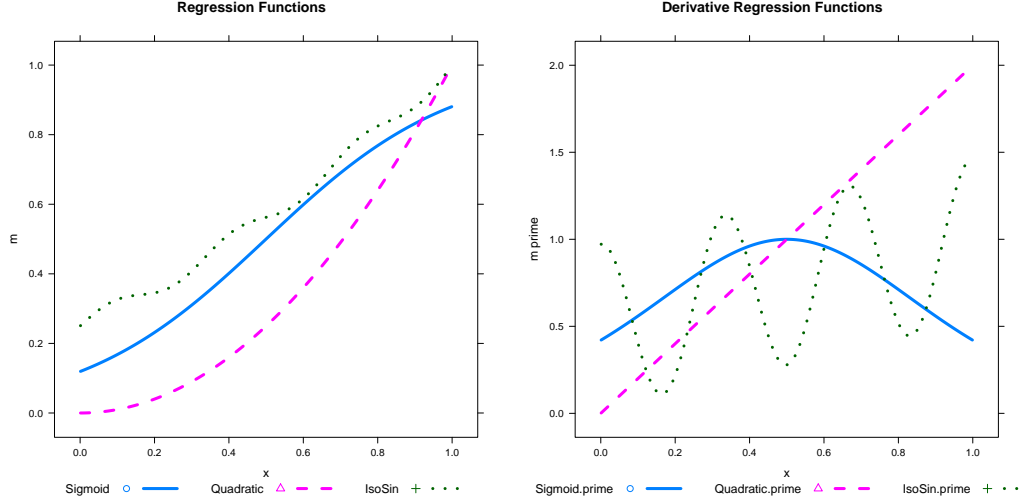


Figure 4: The left plot shows the regression functions: sigmoid, quadratic and isotonic sine functions. The right plot shows their derivatives.

the point that they involve estimates of nuisance parameters, as explained below.

The simulation settings are as follows: the design space is the $[0, 1]$ interval and the regression functions considered: (i) the sigmoid function $m(x) = \exp(4(x - 0.5)) / [1 + \exp(4(x - 0.5))]$, the quadratic function $m(x) = x^2$ and the isotonic sine function $m(x) = (1/40)\sin(6\pi x) + 1/4 + (1/2)x + (1/4)x^2$. The target point d_0 is 0.4, 0.5 or 0.6, while the random error follows a $N(0, \sigma^2)$ distribution, with σ taking values 0.1 and 0.3. The total sample size n ranges from 100 to 500 in increments of 100. All design densities g , g_1 and g_2 are uniform, while the confidence level for all CIs is set to 0.95. The results presented are based on 1000 replicates. For PABLTSP, we set the first stage sample proportions $p = 0.7$ in order obtain accurate coverage rates for all functions. (Yet, as shown in Figure 2, in some cases good coverage rates are achieved at the cost of large average lengths.) For all other two stage procedures, we set p to be the asymptotically optimal proportion of 0.25. The quantiles of \mathbb{D} and \mathcal{Z} for constructing the second-stage sampling intervals for PTSIRP are set to be 4 and 2, respectively, corresponding to $\beta = 0.01$.

When estimating σ and $m'(d_0)$ in the second stage, only Stage 2 points are used in order to stay strictly within the scope of the methods used for these purposes. With smaller budgets as in

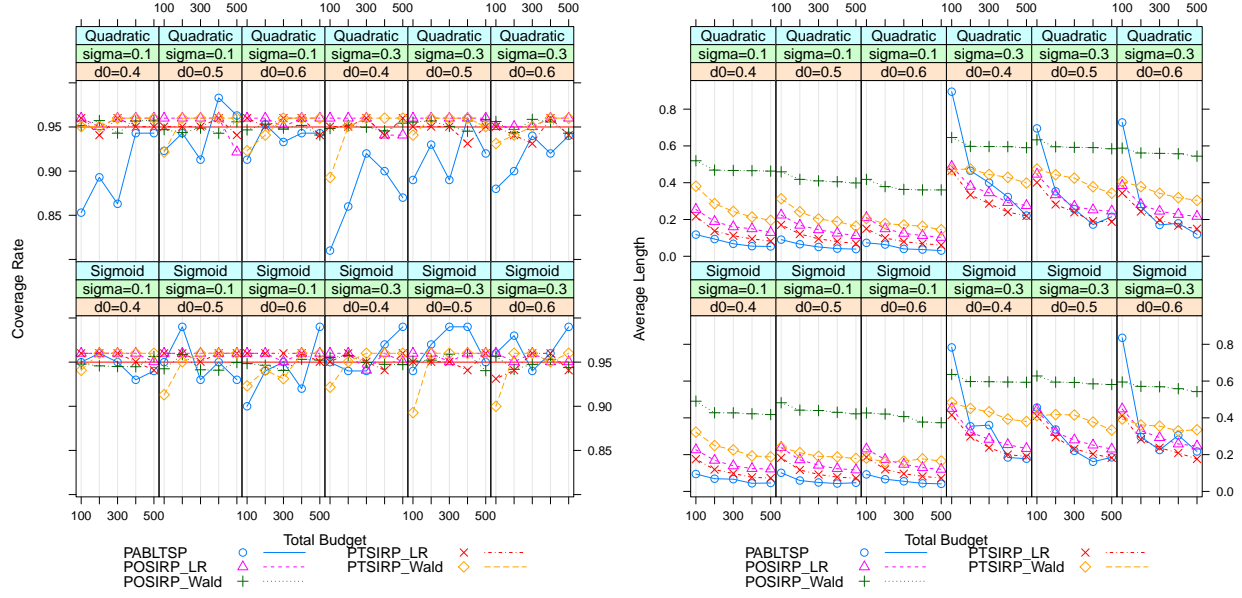


Figure 5: The left and right panels show the coverage rates and average lengths of the 95% confidence intervals for d_0 from the practical procedures with the sigmoid and quadratic functions and different values of σ , d_0 and n .

the real data example, we follow the natural practice of combining both stage samples for updating estimates of σ and $m'(d_0)$, which makes second stage results more reliable.

To gain insight into the simulation results, we depict the plots of the functions under consideration together with their derivatives (see Figure 4).

The coverage rates and average lengths of the 95% confidence intervals for d_0 are shown in Figures 5 and 6.

It can be seen that for the quadratic and sigmoid functions, the proposed two-stage procedures perform well with the coverage being about the nominal level 95% for all d_0 's, sample sizes and noise levels considered. Further, their average lengths are fairly comparable. In contrast, PABLTSP shows inferior performance for larger noise and smaller sample sizes for the quadratic function.

The isotonic sine function proves the most challenging. The left panel of Figure 6 shows the coverage rates of the practical procedures. As discussed in the introduction and seen in the figure, this function exhibits strong nonlinearity causing the the local linear approximation PABLTSP to

feature very poor coverage rates. Also, note that, for the case with $d_0 = 0.5$ the coverage rates of the confidence intervals from POSIRP-Wald and PTSIRP-Wald are consistently lower than 95%. This behavior is caused by inaccurate estimation of $m'(d_0)$ as illustrated in the Supplementary material (Section S2, Figure 1). The true value of $m'(d_0)$ is around 0.279 and the corresponding kernel estimators of $m'(d_0)$ are usually around 0.75, significantly larger than the true value. This makes the confidence interval far too short to cover d_0 and consequently, the coverage rates behave erratically.

Full details for the estimation of $m'(d_0)$, which utilizes a local quadratic regression procedure, are available in Section 4 of [Tang et al. \(2011\)](#). An asymptotically optimal bandwidth, given in equation (3.20) on page 67 of [Fan and Gijbels \(1996\)](#), is employed for this purpose. This local bandwidth minimizes the asymptotic MSE, and indeed with large sample sizes, we find that $m'(d_0)$ is estimated accurately and the coverage rates approach the nominal level. Further emphasizing the importance of the derivative estimate and as illustrated in Figure 2 of the Supplementary material, if we repeat the procedures with perfect knowledge of $m'(d_0)$, then coverage rates are about the nominal level of 95% for the sample sizes considered.

Fortunately, for this wiggly isotonic sine function, POSIRP-LR and PTSIRP-LR have good coverage rates for all simulation cases. This indicates that LR-type confidence intervals are usually robust with different regression functions. The average lengths of the confidence intervals are shown in the right panel of Figure 6. Unsurprisingly, PTSIRP-LR achieves shorter average lengths since it is a two-stage procedure.

In summary, we find that when the underlying regression function is well-behaved, the more aggressive PABLTSP performs well. However, the conservative but stable PTSIRP-LR offers a robust procedure that performs well, even when the underlying function exhibits strong nonlinearities.

4. AN APPLICATION TO FUEL EFFICIENCY STANDARDS

As discussed in Introduction, car fuel efficiency (FE) is an important issue for both manufacturers and consumers, due to new CAFE standards. Note that while the CAFE standards are regulated

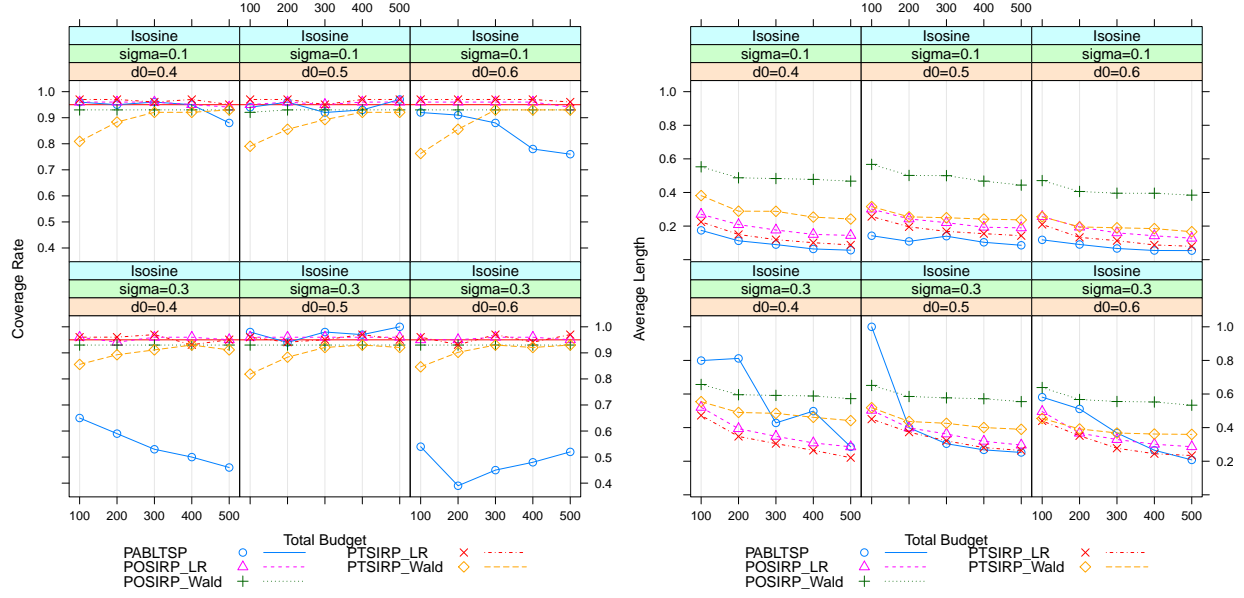


Figure 6: The left panel shows the coverage rates of the 95% confidence intervals for d_0 from the practical procedures with the isotonic sine functions and different values of σ , d_0 and n . The right panel shows the average lengths of the 95% confidence intervals for d_0 .

by the NHTSA, the vehicle FE is assessed by the Environmental Protection Agency (EPA). From 2008 onwards, the EPA measures the fuel efficiency of a vehicle in two testing modes: city and highway, taking into consideration different speeds and acceleration, as well as air conditioning usage and colder outside temperatures, in an effort to better approximate real-world fuel efficiency. From the unadjusted city and highway fuel efficiency, the unadjusted combined fuel efficiency is calculated as follows (see www.epa.gov):

$$\text{Combined FE} = \frac{1}{.495/\text{City FE} + .351/\text{Highway FE}} + .15.$$

The data for this study were extracted from the government website www.fueleconomy.gov that includes all FE data for all 2012 car models available to US consumers. This data set contains the unadjusted city, highway and combined fuel efficiency for 3979 models, together with their horse power. We collected the horse power data for 1477 non-hybrid vehicles with automatic transmission gearboxes and natural aspiration engines (i.e. excluding turbo engines and plug-in hybrid vehicles),

Table 1: Data Analysis Results for the Five Practical Procedures

Procedure	Estimator	“Bias”	95% CI	Coverage	Length	n
POSIRP-Wald	165.022	21.978	[151.595, 178.450]	No	26.855	80
POSIRP-LR	165.022	21.978	[135.887, 301.439]	Yes	165.552	80
PTSIRP-Wald	213.221	26.221	[205.042, 221.400]	No	16.358	40,40
PTSIRP-LR	194.557	7.557	[148.812, 225.955]	Yes	77.143	40,40
PABLTSP	169.509	17.491	[145.982, 172.964]	No	26.982	40,40

in order to have a relatively homogeneous data set.

The objective of our analysis is to estimate the following model $FE = m(HP)$ (or $HP = m^{-1}(FE)$) and then identify the horse power at which the combined FE is equal to 30 MPG, around the 2011 CAFE standard. Hence, we are interested in estimating $d_0 = m^{-1}(30)$.

The scatter plot in the left panel of Figure 1 shows the combined FE of these 1477 vehicles as a function of their horse power and indicates a decreasing relationship. Notice that there are multiple vehicle models with the same horse power, but different FE. To simplify the analysis, we add a small jitter to the original horse power to obtain a unique horsepower for every FE observation, whose scatterplot is given in the right panel of Figure 1. The jitter added is between ± 1 to ensure that the ordering of samples by horsepower remains unchanged.

Given that this is an ‘observed’ data set, we will *emulate* the design setting (for a similar strategy see also Lan et al. (2009)) for a budget of size 80. Both one stage and two stage procedures will be examined. For one stage procedures, 80 horse powers equally spaced are originally selected and the closest ones in the data constitute the final covariate values, together with the corresponding responses. For two stage procedures, we select a portion $p = 0.5$ in the first stage and hence select 40 horse powers in the first stage as previously described. After obtaining the second stage sampling interval (L_1, U_1) we choose with an analogous strategy the remaining 40 points. (Given the relatively modest budget, we chose not to use the asymptotically optimal allocation of 25% + 75%.)

Finally, the “true” value of d_0 is obtained by using isotonic regression on the entire sample of 1477 observations and is estimated to be around 187.

The five procedures considered are: POSIRP-Wald, POSIRP-LR, PTSIRP-Wald, PTSIRP-LR and PABLTSP. The fitted models are shown in Figure 7 and the confidence intervals obtained summarized in Table 1. It is interesting to note that only the LR based procedures produce confidence intervals that cover the “true value.” The two-stage procedure PTSIRP-LR achieves much shorter interval lengths. The PTSIRP-Wald CIs are too short, resulting in their missing the “true value.”

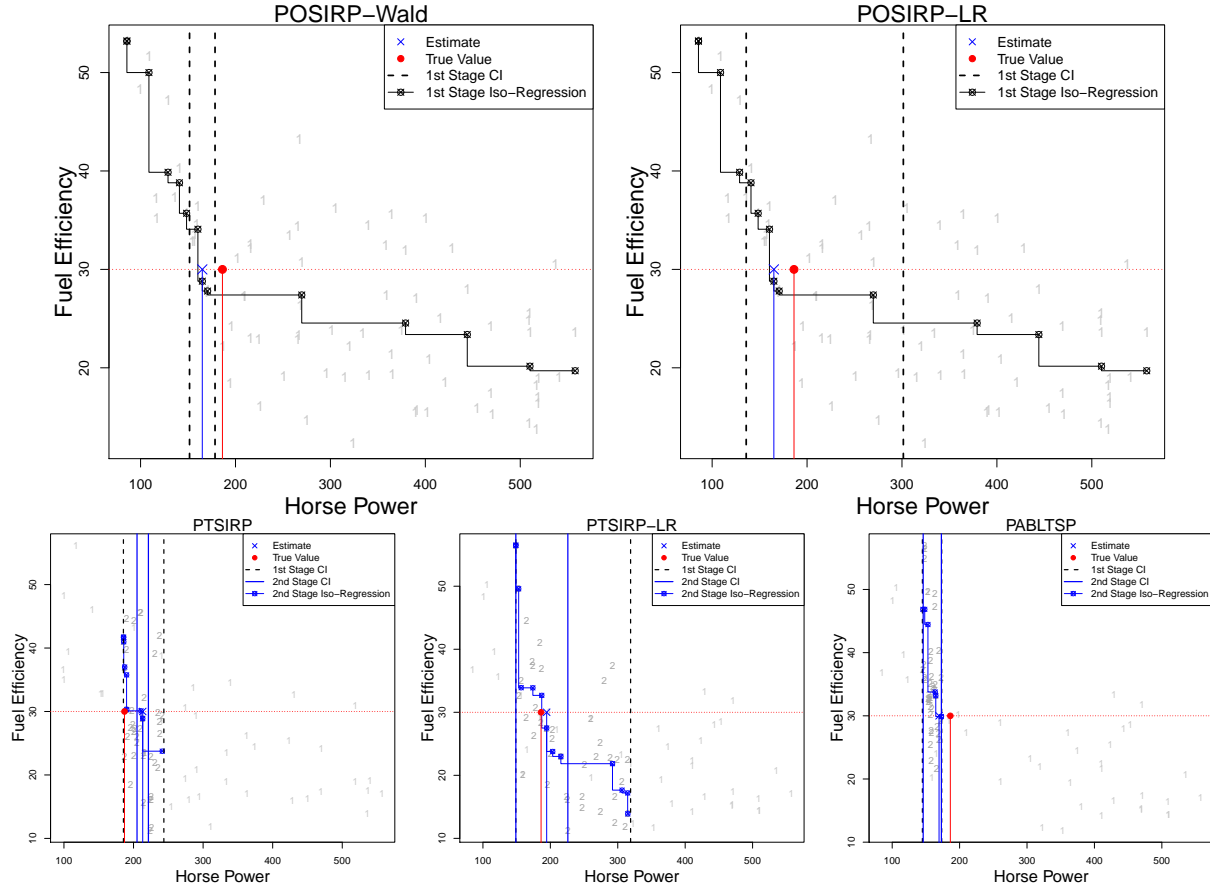


Figure 7: The top panels show one stage procedures: POSIRP-Wald and POSIRP-LR. The bottom panels show two stage procedures: PTSIRP, PTSIRP-LR and PABLTSP. Numbers denote first and second stage samples, vertical lines denote corresponding confidence intervals, and ‘X’ marks the final point estimate.

Additional results from utilizing different allocations in the two stages are provided in Figure

3 of the Supplementary material, where we see that in almost all cases PTSIRP-LR tends to cover the “true” value of 187 with better point estimates. POSIRP-Wald and PTSIRP-Wald continue to struggle due to estimation difficulties with $m'(d_0)$.

Next, we perform another experiment to assess the reliability of the procedures with the FE data set. We treat the data from the 1477 vehicles as the population, and sample from it according to different overall budgets of size 20, 30, 40, 50, 60, 70, 80, 90, 100. Given the modest budgets, we combine samples from both stages for estimation of auxiliary parameters and inversion of the likelihood ratio. The results, averaged over 500 repetitions for each budget size, are depicted in Figure 8. Note that POSIRP-Wald and PTSIRP-Wald still struggle to maintain coverage rates due to difficulties of auxiliary parameter estimation. The local linear approximation in PABLTSP also faces difficulties with such small budgets. On the other hand, POSIRP-LR and PTSIRP-LR maintain good coverage for all budgets. As noted before, PTSIRP-LR outperforms its one-stage counterpart with narrower intervals. Considering the overall budgets investigated in this experiment, PTSIRP-LR performs well with an extremely small fraction of the overall data, illustrating its utility in the context of very large data sets, a topic of further discussion in the Discussion section.

Finally, we return to the task discussed in the introductory section of estimating the horse power at which the combined FE is equal to the upcoming 2016 CAFE standard of $d_0 = m^{-1}(34)$. Employing isotonic regression on the entire sample yields a “true” value of d_0 of around 155, with corresponding 95% confidence interval [143.360, 166.052]. Following the same procedure and budget allocations as above, PTSIRP-LR yields $\hat{d}_0 = 166.204$ with corresponding 95% confidence interval [145.599, 175.450], as shown in Figure 9. PTSIRP-LR covers the “true” value with a reasonably sized interval, while utilizing a small fraction of the overall budget.

The upshot of the analysis is that the two stage LR based procedure offers superior performance to its competitors even with smaller budgets and when the underlying function exhibits nonlinearities.

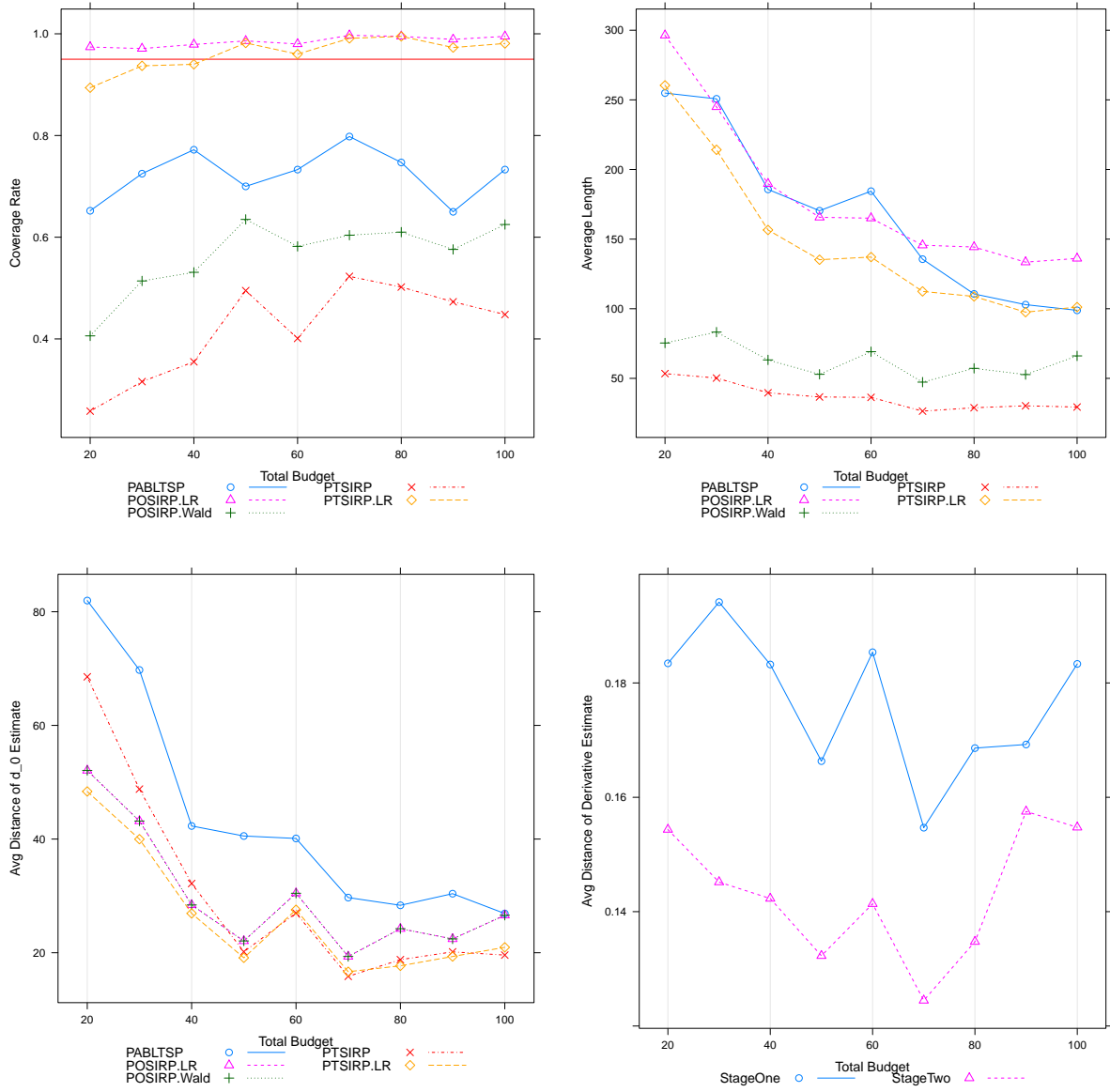


Figure 8: Results obtained after combining both stage samples. The top panel shows the coverage rate and average length of confidence intervals generated by the five different procedures. The bottom panel shows the distance of the point estimate to the “true” value, and the distance of the derivative estimate to its “true” value.

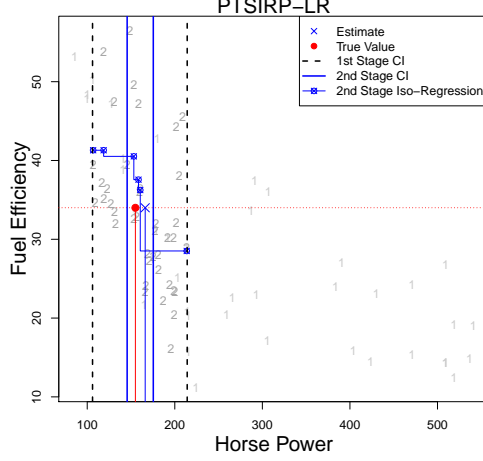


Figure 9: PTSIRP-LR results for estimating the 2016 CAFE standard of $d_0 = m^{-1}(34)$. Numbers denote first and second stage samples, vertical lines denote corresponding confidence intervals, and ‘X’ marks the final point estimate.

5. DISCUSSION AND CONCLUDING REMARKS

In this paper, we considered the estimation of the inverse of a monotone regression function at a given point in a design setting. The results strongly suggest that a two-stage procedure using isotonic regression in both stages coupled with calculation of likelihood-ratio based confidence intervals is agnostic to the local structure in the vicinity of the parameter of interest, requires minimal tuning and exhibits superior performance.

The reader may wonder whether an alternative nonparametric procedure at stage one, with a faster than the $n^{1/3}$ convergence rate of isotonic regression may offer advantages to the proposed strategy. We have investigated smoothed isotonic regression (Tang, 2011) which, in a single stage, exhibits a convergence rate of $n^{2/5}$ and when repeated in the second stage exhibits the same acceleration pattern as isotonic regression provided the bandwidth is appropriately chosen (for a detailed discussion of this subtle issue see (Tang, 2011)). However, extensive numerical work shows that no significant performance gains are realized, compared to using isotonic regression in both stages, while at the same time a bandwidth parameter needs to be carefully specified. Indeed, a strategy based on isotonic regression in the first stage, followed by smooth isotonic regression in

the second stage struggles with the estimation of the iso-sine function presented in Figure 2.

Finally, we should note that although the developed methodology applies to design settings (where the investigator can select the desired covariate and the corresponding response variable values), it can also prove useful in the context of very large data sets. Suppose that one is interested in estimating a threshold of a monotone function from a very large data set that can not be stored in its entirety in computer memory. In that case, one-stage estimation based on the entire data set is computationally challenging, since it requires appropriate modification of the standard algorithms. However, by adopting the proposed adaptive design framework, one can overcome such computational difficulties, while still obtaining a high degree of accuracy. It is our belief that by going to multiple stages, if necessary, with judiciously chosen parameters, one can match the performance of the estimator based on all data that could be stored in computer memory, thus providing a computationally efficient procedure that avoids major modifications of existing algorithms. The latter claim is supported by the results of the experiment shown in Figure 8, and in Figure 4 of the Supplementary material, which indicates the PTSIRP-LR reduces computing time by substantial amounts at larger budgets compared to its one stage counterpart.

APPENDIX A. PROOFS

We discuss Propositions 1 and 2 of the paper.

A.1 Appendix of TSIRP

We introduce the following *idealized* two-stage isotonic regression procedure (ITSIRP) as follows:

1. Set the first-stage sample proportion $p \in (0, 1)$ and let the first and second-stage sample sizes be $n_1 = \lfloor np \rfloor$ and $n_2 = n - n_1$, respectively, where n is the total sample size.
2. Let the ideal second-stage sampling interval be $[L_{1i}, U_{1i}] = [d_0 \pm C_1 n_1^{-\gamma_1}]$ with $C_1 > 0$ and $\gamma_1 > 0$.
3. Allocate the second-stage design points $\{X_{2,i}\}_{i=1}^{n_2}$ according to a Lebesgue density \tilde{g}_2 on $[L_{1i}, U_{1i}]$, given by $\tilde{g}_2(x) = (C_1 n_1^{-\gamma_1})^{-1} \psi((x - d_0)/(C_1 n_1^{-\gamma_1}))$. Denote the corresponding i.i.d.

second-stage responses $\{Y_{2,i}\}_{i=1}^{n_2}$.

4. Compute the unconstrained isotonic regression m_{oI} (and the constrained one m_{oIc} under the null hypothesis $m^{-1}(\theta_0) = d_0$) of m over $[L_{1i}, U_{1i}]$ from the second-stage data.
5. Obtain $d_{oI} = m_{oI}^{-1}(\theta_0)$ and $2 \log \lambda_{oI} = 2 \log \lambda_{oI}(d_0) = 2[l_n(m_{oI}, \hat{\sigma}) - l_n(m_{oIc}, \hat{\sigma})]$, the ideal second-stage isotonic regression based estimator of d_0 and likelihood ratio statistic under $H_0 : m^{-1}(\theta_0) = d_0$; here, as before, $\hat{\sigma}$ is a consistent estimate of σ .

Remark: Note that ITSIRP is similar to TSIRP except that in ITSIRP the second-stage sampling interval is centered at d_0 instead of at $d_{1,I}$; therefore, the sampling density at Stage 2 in ITSIRP is ψ renormalized to $[L_{1i}, U_{1i}]$, just as g_2 is ψ renormalized to $[L_1, U_1]$ (see Proposition 1) in TSIRP. Since $d_{1,I}$ converges to d_0 at rate $n^{1/3}$, which is faster than the rate at which $[L_1, U_1]$ is decreasing around $d_{1,I}$ (since $\gamma < 1/3$), $[L_1, U_1]$ is essentially indistinguishable from its idealized counterpart $[L_{1i}, U_{1i}]$ and the asymptotic behavior of d_{oI} will be *identical* to that of d_{2I} . Similarly, the asymptotic distribution of the idealized LRT, $2 \log \lambda_{oI}$, will be the *same* as that of $2 \log \lambda_{2,I}$.

A rigorous proof of Proposition 1, formalizing the intuition above, can be provided via conditioning arguments similar in spirit to those used for proving Theorem 2 in Lan (2007) that establishes the distributional convergence of the two-stage estimator of a change-point in a regression model; more specifically, the proof of Lemma 3.2 (a key intermediate step in proving Theorem 2) of a process convergence result proceeds by conditioning on the values of the relevant estimates at Stage 1 in conjunction with some uniformity arguments. Proposition 2 requires similar conditioning strategies. In this paper, we provide a sketch of the derivations of the limiting distributions of the ‘idealized’ (surrogate) quantities d_{oI} and $2 \log \lambda_{oI}$. We first introduce the following quantities.

For positive constants a, b we define the process $X_{a,b}(t) \equiv aW(t) + bt^2$ where $W(t)$ is two-sided Brownian motion on \mathbb{R} , starting from 0. For a function f defined on \mathbb{R} , let $\text{slogcm}(f, I)$ denote the left slope of the greatest convex minorant of the restriction of f to the interval I . Define $g_{a,b}(t) = \text{slogcm}(X_{a,b}, \mathbb{R})(t)$ and $g_{a,b}^0(t) = \{\text{slogcm}(X_{a,b}, (-\infty, 0])(t) \wedge 0\} 1(t \leq 0) + \{\text{slogcm}(X_{a,b}, (0, \infty])(t) \vee$

$0\} 1(t > 0)$. Define $\mathbb{D} = \int \{(g_{1,1}(t))^2 - (g_{1,1}^0(t))^2\} dt$ and recall that $\mathcal{Z} \equiv \text{Argmin}_t X_{1,1}(t)$ is the Chernoff random variable.

Theorem 3. *Under Assumption A, we have*

$$n^{(1+\gamma_1)/3}(d_{oI} - d_0) \xrightarrow{d} C_{d_{oI}} \mathcal{Z},$$

$$\text{where } C_{d_{oI}} = C_{d_I} \left(\frac{C_1}{(1-p)p^{\gamma_1}\psi(0)} \right)^{1/3}.$$

Theorem 4. *Under Assumption A and the null hypothesis $H_0 : m^{-1}(\theta_0) = d_0$, $2 \log \lambda_{oI} \xrightarrow{d} \mathbb{D}$.*

Proof-sketch of Theorem 3. For every $x \in \mathbb{R}$,

$$\begin{aligned} P \left(n_2^{(1+\gamma_1)/3}(d_{oI} - d_0) \leq x \right) &= P \left(d_{oI} \leq d_0 + x n_2^{-(1+\gamma_1)/3} \right) \\ &= P \left(\theta_0 \leq m_{oI}(d_0 + x n_2^{-(1+\gamma_1)/3}) \right) \\ &= P \left(n_2^{(1+\gamma_1)/3}(m_{oI}(d_0 + x n_2^{-(1+\gamma_1)/3}) - \theta_0) \geq 0 \right) \quad (\text{A1}) \\ &= P \left(n_2^{(1+\gamma_1)/3}(m_{oI}(d_0 + x n_2^{-(1+\gamma_1)/3}) - m(d_0)) \geq 0 \right). \quad (\text{A2}) \end{aligned}$$

Thus, it is sufficient to derive the limiting distribution of $n_2^{(1+\gamma_1)/3}(m_{oI}(d_0 + x n_2^{-(1+\gamma_1)/3}) - m(d_0))$. Deducing this limit involves three main steps: the first uses a switching relationship to change the original problem into an M-Estimation problem; the second solves the M-Estimation problem in the framework of empirical process theory; the third simplifies the final limit distribution. This approach is, by now, standard in dealing with the asymptotics of isotonic estimates; see, for example, pages 296-299 of [van der Vaart and Wellner \(1996\)](#). Without loss of generality, we take $[a, b] =]0, 1]$ from here on.

In the first step, we show

Lemma 5. *For $t \in [d_0 \pm C_1 n_1^{-\gamma_1}]$ and $s \in \mathbb{R}$,*

$$m_{oI}(t) \leq s \Leftrightarrow \underset{x \in [d_0 \pm C_1 n_1^{-\gamma_1}]}{\text{argmin}} \{V_{n_2}(x) - s G_{n_2}(x)\} \geq T(t), \quad (\text{A3})$$

where,

$$V_{n_2}(x) = \frac{1}{n_2} \sum_{i=1}^{n_2} Y_{2,i} 1(X_{2,i} \leq x), \quad G_{n_2}(x) = \frac{1}{n_2} \sum_{i=1}^{n_2} 1(X_{2,i} \leq x); \quad (\text{A4})$$

$T(t)$ is the largest $X_{2,i}$ less than or equal to t .

This equivalence is called the ‘switching relationship’ and can be derived by arguments similar to those leading to the last display on page 298 of van der Vaart and Wellner (1996). Hence,

$$\begin{aligned} & P\left(n_2^{(1+\gamma_1)/3}(m_{oI}(d_0 + xn_2^{-(1+\gamma_1)/3}) - m(d_0)) \leq z\right) \\ &= P\left(m_{oI}(d_0 + xn_2^{-(1+\gamma_1)/3}) \leq m(d_0) + zn_2^{-(1+\gamma_1)/3}\right) \\ &= P\left(\underset{x \in [d_0 \pm C_1 n_1^{-\gamma_1}]}{\operatorname{argmin}} \left\{V_{n_2}(x) - (m(d_0) + zn_2^{-(1+\gamma_1)/3})G_{n_2}(x)\right\} \geq T(d_0 + xn_2^{-(1+\gamma_1)/3})\right). \end{aligned}$$

In the second step, by arguments similar to those on Page 299 of van der Vaart and Wellner (1996), we establish:

Lemma 6. *Under Assumption (A), as $n \rightarrow \infty$,*

$$\begin{aligned} & P\left(\underset{x \in [d_0 \pm C_1 n_1^{-\gamma_1}]}{\operatorname{argmin}} \left\{V_{n_2}(x) - (m(d_0) + zn_2^{-(1+\gamma_1)/3})G_{n_2}(x)\right\} \geq T(d_0 + xn_2^{-(1+\gamma_1)/3})\right) \\ & \rightarrow P\left(\underset{h \in \mathbb{R}}{\operatorname{argmin}} \{X_{c,d} - zh\} \geq x\right), \end{aligned}$$

where $c = (C_1 \sigma^2 ((1-p)/p)^\gamma / \psi(0))^{1/2}$ and $d = m'(d_0)/2$.

In the third step, we use another switching relationship, namely:

$$g_{c,d}(x) > \lambda \iff \underset{t \in \mathbb{R}}{\operatorname{argmin}} (X_{c,d}(t) - \lambda t) < x, \quad \text{for } \lambda \in \mathbb{R}, \quad (\text{A5})$$

and the continuity of the random variables involved in the above display, to get:

$$P\left(\underset{h \in \mathbb{R}}{\operatorname{argmin}} \{X_{c,d} - zh\} \geq x\right) = P(g_{c,d}(x) \leq z).$$

Hence,

$$n_2^{(1+\gamma_1)/3}(m_{oI}(d_0 + xn_2^{-(1+\gamma_1)/3}) - m(d_0)) \rightarrow_d g_{c,d}(x) \quad (\text{A6})$$

It follows from (A1) that

$$P(n_2^{(1+\gamma_1)/3}(d_{oI} - d_0) \leq x) \rightarrow P(g_{c,d}(x) \geq 0). \quad (\text{A7})$$

Then, using (A5) again, we have

$$P\left(n_2^{(1+\gamma_1)/3}(d_{oI} - d_0) \leq x\right) \rightarrow P\left(\underset{t \in \mathbb{R}}{\operatorname{argmin}} X_{c,d}(t) \leq x\right). \quad (\text{A8})$$

Now, from Problem 5 on Page 308 of van der Vaart and Wellner (1996), we have $\arg \min X_{c,d}(h) = (c/d)^{2/3} \arg \min X_{1,1}(t)$, whence

$$P\left(n_2^{(1+\gamma_1)/3}(d_{oI} - d_0) \leq x\right) \rightarrow P\left((c/d)^{2/3} \underset{t \in \mathbb{R}}{\operatorname{argmin}} X_{1,1}(t) \leq x\right). \quad (\text{A9})$$

Since

$$(c/d)^{2/3} = \left(\frac{4\sigma^2}{m'(d_0)^2} \cdot \frac{(1-p)^{\gamma_1} C_1}{p^{\gamma_1} \psi(0)} \right)^{1/3},$$

we have

$$n_2^{(1+\gamma_1)/3}(d_{oI} - d_0) \xrightarrow{d} C_{d_I} \left(\frac{(1-p)^{\gamma_1} C_1}{p^{\gamma_1} \psi(0)} \right)^{1/3} \mathcal{Z},$$

which leads to $n^{(1+\gamma_1)/3}(d_{oI} - d_0) \xrightarrow{d} C_{d_{oI}} \mathcal{Z}$, the result in Theorem 3. \square

Proof-sketch of Theorem 4. For simplicity, we assume the second-stage sampling density is uniform on $[L_{1i}, U_{1i}]$. That is, $g_2(x) = (2C_1 n_1^{-\gamma_1})^{-1}$ for $x \in [L_{1i}, U_{1i}]$. Then, similar to (A6), we have

$$\begin{pmatrix} n_2^{(1+\gamma_1)/3}(m_{oI}(d_0 + x n_2^{-(1+\gamma_1)/3}) - m(d_0)) \\ n_2^{(1+\gamma_1)/3}(m_{oIc}(d_0 + x n_2^{-(1+\gamma_1)/3}) - m(d_0)) \end{pmatrix} \xrightarrow{d} \begin{pmatrix} g_{c,d}(x) \\ g_{c,d}^o(x) \end{pmatrix}, \quad (\text{A10})$$

where now, $c = (2C_1 \sigma^2 [(1-p)/p]^{\gamma_1})^{1/2}$ and $d = m'(d_0)/2$. In fact, the weak convergence (A10) holds not only finite dimensionally, but also in the normed linear space $L_2[-K, K] \times L_2[-K, K]$ for every $K > 0$, because of the monotonicity of both m_{oI} and m_{oIc} .

To derive the asymptotics for $2 \log \lambda_{oI}$, it suffices (by Slutsky's theorem) to consider a tweaked version of this quantity with the $\hat{\sigma}^2$ in the denominator replaced by the true σ^2 . In what follows,

we work with this version and continue to call it $2 \log \lambda_{oI}$. We have:

$$\begin{aligned}
2 \log \lambda_{oI} &= 2 \left[\frac{1}{2\sigma^2} \sum_{i=1}^{n_2} (Y_{2,i} - m_{oIc}(X_{2,i}))^2 - \frac{1}{2\sigma^2} \sum_{i=1}^{n_2} (Y_{2,i} - m_{oI}(X_{2,i}))^2 \right] \\
&= \frac{1}{\sigma^2} \left\{ \sum_{i=1}^{n_2} [(Y_{2,i} - \theta_0) - (m_{oIc}(X_{2,i}) - \theta_0)]^2 - \sum_{i=1}^{n_2} [(Y_{2,i} - \theta_0) - (m_{oI}(X_{2,i}) - \theta_0)]^2 \right\} \\
&= -\frac{2}{\sigma^2} \left[\sum_{i=1}^{n_2} (Y_{2,i} - \theta_0)(m_{oIc}(X_{2,i}) - \theta_0) - \sum_{i=1}^{n_2} (Y_{2,i} - \theta_0)(m_{oI}(X_{2,i}) - \theta_0) \right] \\
&\quad + \frac{1}{\sigma^2} \sum_{i=1}^{n_2} [(m_{oIc}(X_{2,i}) - \theta_0)^2 - (m_{oI}(X_{2,i}) - \theta_0)^2] \\
&= -\frac{2}{\sigma^2} \sum_{i=1}^{n_2} (Y_{2,i} - m_{oIc}(X_{2,i}))(m_{oIc}(X_{2,i}) - \theta_0) - \frac{2}{\sigma^2} \sum_{i=1}^{n_2} (m_{oIc}(X_{2,i}) - \theta_0)^2 \\
&\quad + \frac{2}{\sigma^2} \sum_{i=1}^{n_2} (Y_{2,i} - m_{oI}(X_{2,i}))(m_{oI}(X_{2,i}) - \theta_0) + \frac{2}{\sigma^2} \sum_{i=1}^{n_2} (m_{oI}(X_{2,i}) - \theta_0)^2 \\
&\quad + \frac{1}{\sigma^2} \sum_{i=1}^{n_2} [(m_{oIc}(X_{2,i}) - \theta_0)^2 - (m_{oI}(X_{2,i}) - \theta_0)^2] \\
&= \frac{1}{\sigma^2} \sum_{i=1}^{n_2} [(m_{oI}(X_{2,i}) - \theta_0)^2 - (m_{oIc}(X_{2,i}) - \theta_0)^2],
\end{aligned}$$

where the last equation is a consequence of the fact that isotonic regression estimators are formed by averaging the responses over blocks of order statistics of the covariates, which ensures that

$$\sum_{i=1}^{n_2} (Y_{2,i} - m_{oI}(X_{2,i}))(m_{oI}(X_{2,i}) - \theta_0) \quad \text{and} \quad \sum_{i=1}^{n_2} (Y_{2,i} - m_{oIc}(X_{2,i}))(m_{oIc}(X_{2,i}) - \theta_0)$$

are both equal to 0.

Now denote \mathbb{P}_{n_2} as the empirical measure of the second-stage covariates $\{X_{2,i}\}_{i=1}^{n_2}$ and P_{n_2} as the corresponding uniform probability measure of $X_{2,i}$. Let D_{n_2} denote the interval on which m_{oI} and m_{oIc} differ. Then, we have

$$2 \log \lambda_{oI} = \frac{n_2}{\sigma^2} \mathbb{P}_{n_2} [(m_{oI}(x) - \theta_0)^2 - (m_{oIc}(x) - \theta_0)^2] \{x \in D_{n_2}\} = T_1 + T_2,$$

where

$$\begin{aligned}
T_1 &= \frac{n_2}{\sigma^2} (\mathbb{P}_{n_2} - P_{n_2}) [(m_{oI}(x) - \theta_0)^2 - (m_{oIc}(x) - \theta_0)^2] \{x \in D_{n_2}\}, \\
T_2 &= \frac{n_2}{\sigma^2} P_{n_2} [(m_{oI}(x) - \theta_0)^2 - (m_{oIc}(x) - \theta_0)^2] \{x \in D_{n_2}\}.
\end{aligned}$$

Since $(1 - 2\gamma_1)/3 < 1/2$, both $(m_{oI}(x) - \theta_0)$ and $(m_{oIc}(x) - \theta_0)$ are $O_P(n_2^{\frac{1+\gamma_1}{3}})$ and

$$T_1 = \frac{1}{\sigma^2} n_2^{\frac{1-2\gamma_1}{3}} (\mathbb{P}_{n_2} - P_{n_2}) \left\{ \left[n_2^{\frac{1+\gamma_1}{3}} (m_{oI}(x) - \theta_0) \right]^2 - \left[n_2^{\frac{1+\gamma_1}{3}} (m_{oIc}(x) - \theta_0) \right]^2 \right\} \{x \in D_{n_2}\},$$

we can show that T_1 converges to 0 in probability by empirical process theory arguments.

Next, T_2 is given by

$$\begin{aligned} & \frac{n_2}{\sigma^2} \int_{D_{n_2}} [(m_{oI}(x) - \theta_0)^2 - (m_{oIc}(x) - \theta_0)^2] \frac{n_1^{\gamma_1}}{2C_1} dx \\ &= \frac{1}{2C_1\sigma^2} \left(\frac{p}{1-p} \right)^{\gamma_1} n_2^{1+\gamma_1} \int_{D_{n_2}} [(m_{oI}(x) - \theta_0)^2 - (m_{oIc}(x) - \theta_0)^2] dx \\ &= \frac{1}{c^2} n_2^{1+\gamma_1} \int_{D_{n_2}} [(m_{oI}(x) - \theta_0)^2 - (m_{oIc}(x) - \theta_0)^2] dx \\ &= \frac{1}{c^2} \int_{n_2^{\frac{1+\gamma_1}{3}}(D_{n_2}-d_0)} \left\{ \left[n_2^{\frac{1+\gamma_1}{3}} (m_{oI}(d_0 + tn_2^{-\frac{1+\gamma_1}{3}}) - \theta_0) \right]^2 - \left[n_2^{\frac{1+\gamma_1}{3}} (m_{oIc}(d_0 + tn_2^{-\frac{1+\gamma_1}{3}}) - \theta_0) \right]^2 \right\} dt \\ &\xrightarrow{d} \frac{1}{c^2} \int [g_{c,d}(t)^2 - g_{c,d}^o(t)^2] dt = \mathbb{D}. \end{aligned}$$

The equality preceding the weak convergence above follows from the change of variable $x = d_0 + tn_2^{-(1+\gamma_1)/3}$ and the weak convergence of the likelihood ratio statistic follows from the weak convergence result (A10) in the L_2 sense and the fact that the set $n_2^{\frac{1+\gamma_1}{3}}(D_{n_2} - d_0)$ is contained in a compact set with (arbitrarily) high probability, eventually. For the very last equality, see, for example, the proof of Theorem 2.2 of Banerjee (2007). Thus, Theorem 4 holds. □

REFERENCES

- Banerjee, M. (2000), Likelihood Ratio Inference in Regular and Non-regular Problems, PhD thesis, University of Washington.
- Banerjee, M. (2007), “Likelihood based inference for monotone response models,” *Annals of Statistics*, 35, 931–956.
- Banerjee, M. (2009), “Inference in exponential family regression models under certain shape constraints,” in *Advances in Multivariate Statistical Methods, Statistical Science and Interdisciplinary Research*, Vol. 4 World Scientific, pp. 249–272.

- Banerjee, M., and Wellner, J. (2001), “Likelihood Ratio Tests for Monotone Functions,” *Annals of Statistics*, 29, 1699 – 1731.
- Fan, J., and Gijbels, I. (1996), *Local polynomial modelling and its applications*, Vol. 66 of *Mono-graphs on Statistics and Applied Probability*, London: Chapman & Hall.
- Gasser, T., Sroka, L., and Jennen-Steinmetz, C. (1986), “Residual variance and residual pattern in nonlinear regression,” *Biometrika*, 73(3), 625–633.
- Groeneboom, P., and Wellner, J. A. (2001), “Computing Chernoff’s distribution,” *J. Comput. Graph. Statist.*, 10(2), 388–400.
- Lan, Y. (2007), Topics on change-point estimation under adaptive sampling procedures, PhD thesis, University of Michigan.
- Lan, Y., Banerjee, M., and Michailidis, G. (2009), “Change-point estimation under adaptive sampling,” *The Annals of Statistics*, 37(4), 1752–1791.
- Osborne, C. (1991), “Statistical Calibration: A Review,” *International Statistical Review*, 59, 309–336.
- Rosenberger, W. F., and Haines, L. M. (2002), “Competing designs for phase I clinical trials: a review,” *Stat. Med.*, 21, 2757–2770.
- Tang, R. (2011), Adaptive and Multistage Procedures for Inference on Monotone Regression Functions in Observed Data Studies and Design Settings, PhD thesis, University of Michigan.
- Tang, R., Banerjee, M., and Michailidis, G. (2011), “A two-stage hybrid procedure for estimating an inverse regression function,” *The Annals of Statistics*, 39, 956–989.
- van der Vaart, A. W., and Wellner, J. A. (1996), *Weak Convergence and Empirical Processes* Springer.

Two-Stage Plans for Estimating a Threshold Value of a Regression Function: Supplemental Technical Material

RUNLONG TANG¹, MOULINATH BANERJEE², GEORGE MICHAILIDIS², AND SHAWN MANKAD²

¹*Department of Operations Research and Financial Engineering, Princeton University*

²*Department of Statistics, University of Michigan*

S1. MULTISTAGE ADAPTIVE PROCEDURE AND ITS CONVERGENCE RATE

Next, we discuss whether the parametric convergence rate of \sqrt{n} can be achieved by using a multistage sampling procedure (with more than 2 stages) that constructs an isotonic regression estimate of d_0 at each stage. So, consider the generic adaptive procedure described at the beginning of Section 2.2 where we obtain $d_{2,I}$ by IR at Step 4 but instead of finding a confidence interval in Step 5, we select a neighborhood of $d_{2,I}$, say $[L_2, U_2]$, and continue sampling at Stage 3. Of course, in this case, we allocate our budget in proportions p_1, p_2, p_3 adding up to 1. Now, the convergence rate of $d_{2,I}$ for d_0 is $n^{(1+\gamma_1)/3}$ and $[L_2, U_2]$ is therefore chosen to be of the form $[d_{2,I} \pm C_2 n_2^{-\gamma_2}]$, with $\gamma_2 < (1 + \gamma_1)/3$ and $n_2 \equiv n p_2$. Since $\gamma_1 < 1/2$, we have $\gamma_2 < 1/2$. Finally, $n_3 \equiv n p_3$ covariate-response pairs are sampled from $[L_2, U_2]$ at Stage 3 and the IR procedure is used to come up with a final estimate $d_{3,I}$ with convergence rate $n^{(1+\gamma_2)/3}$. But, as $(1 + \gamma_2)/3 < 1/2$, this is again slower than \sqrt{n} . Following this line of argument, it is not difficult to see that no k -stage procedure based on IR at each stage can produce an estimator of d_0 that achieves the parametric rate. Note, also, that we can

come as close as possible to \sqrt{n} if k is chosen large enough. A k -stage procedure involves a sequence $(\gamma_1, \gamma_2, \dots, \gamma_{k-1})$ with $1/2 > \gamma_1$ and $\gamma_{i+1} < (1 + \gamma_i)/3$, for $i \geq 1$ and yields a final rate of convergence given by $(1 + \gamma_{k-1})/3$. Now, take some large k and consider a procedure where $(1 + \gamma_{i-1})/3 > \gamma_i > (1 + \gamma_{i-1})/3 - \eta$ for some (very small) $\eta > 0$, for $i = k, (k-1), \dots, 2$. Then, using the second inequality time and again, by simple algebra:

$$\frac{(1 + \gamma_{k-1})}{3} > (1 - \eta) \sum_{j=1}^{k-2} \left(\frac{1}{3}\right)^j + \left(\frac{1}{3}\right)^{k-1} + \frac{\gamma_1}{3^{k-1}},$$

which can clearly be made as close to $1/2$ as one pleases for small (enough) η and large (enough) k .

S2. SUPPLEMENTAL MATERIAL FOR PERFORMANCE EVALUATION OF THE ADAPTIVE PROCEDURES

In this section we will present additional results regarding the estimation of $m'(d_0)$.

We use a local quadratic regression procedure to estimate $m'(d_0)$. An asymptotically optimal bandwidth that minimizes the asymptotic MSE is employed for this purpose. As expected and shown in Figure 1, the estimator tends to perform well with very large sample sizes. However, for the sample sizes considered in our numerical work, the performance is unsatisfactory especially under the isotonic sine function. The root mean squared error can be substantial, which causes the coverage rates reported in the main text to behave erratically.

If we repeat the procedures with perfect knowledge of the nuisance parameter $m'(d_0)$, then coverage rates are about the nominal level of 95% (Figure 2). Therefore, when the underlying regression function is well-behaved, we can use the more aggressive PTSIRP. Otherwise, we use the conservative but stable PTSIRP-LR, which avoids derivative estimation.

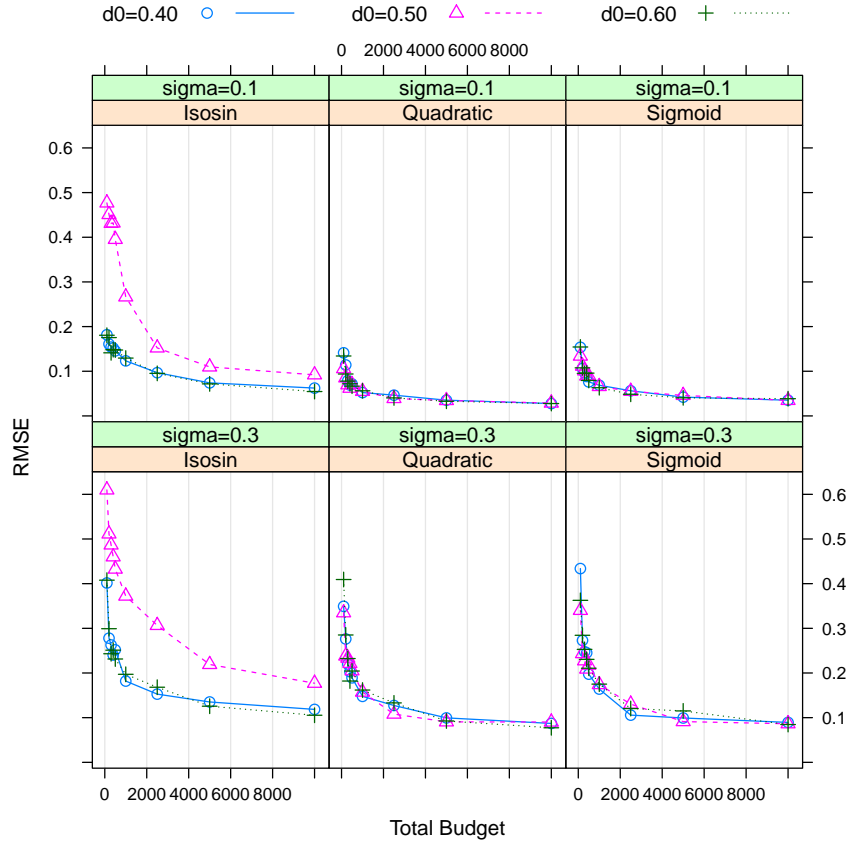


Figure 1: This figure shows the root mean squared errors of the estimates of $m'(d_0)$ using the local quadratic regression procedure proposed in Fan and Gijbels (1996). The first five data points correspond to sample sizes considered, e.g., sample sizes of 100,200,...,500.

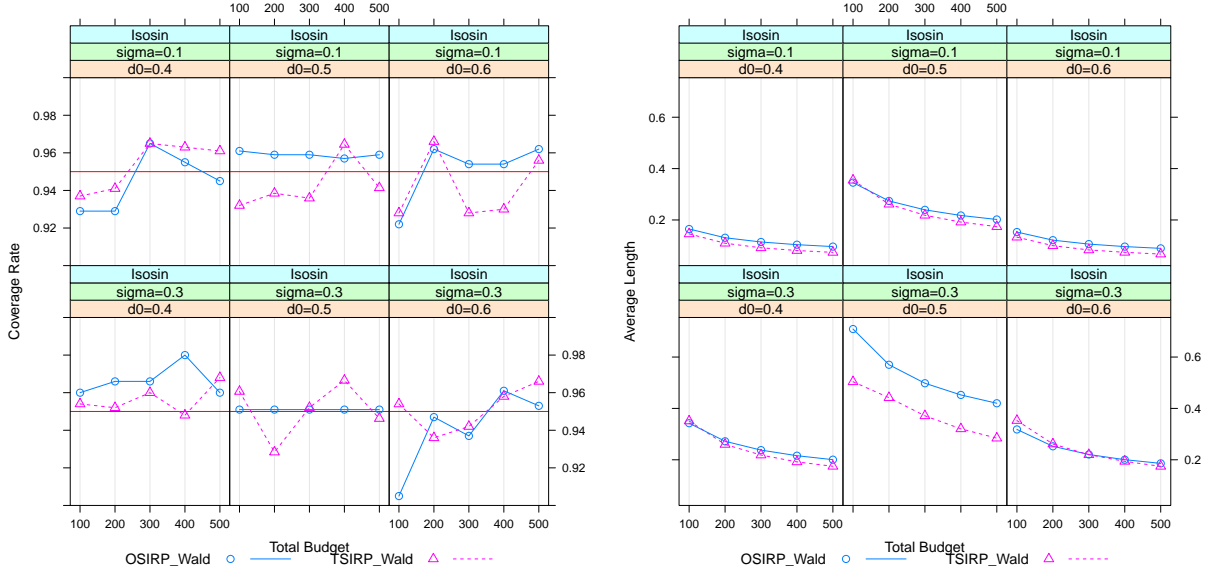


Figure 2: The left panel shows the coverage rates of the 95% confidence intervals for $d_0 = 0.5$ from the one and two stage IR-wald procedures with the isotonic sine functions and different values of σ and n . The right panel shows the average lengths of the 95% confidence intervals for d_0 . The derivative $m'(d_0)$ and σ are assumed known.

S3. DIFFERENT BUDGET ALLOCATIONS FOR FUEL EFFICIENCY ANALYSIS

In this section, we repeat the analysis from the main text with different budget specifications. In particular, we present in Figure 3 three different scenarios maintaining the total budget of 80 samples.

Note that the one-stage procedures tend to provide poor point estimates. Whereas, the LR based two stage procedure PTSIRP-LR and the local linear approximation (PABLTSP) tend to cover the “true” value of 187 in almost all cases with better point estimates.

In addition to providing reliable estimates with smaller budgets and ‘ill-behaved’ functions, PTSIRP-LR reduces computing time by substantial amounts at larger budgets compared to its one stage counterpart. Figure 4 shows computing times, averaged over 500 trials, with 50% of the overall budget allocated to the first stage for every trial. The Wald and local linear procedures can be performed faster, though their efficacy is dubious with smaller budgets and with ‘ill-behaved’ functions due to auxiliary parameters estimation.

Altogether, our numerical studies have shown that likelihood ratio based procedures are robust, but do require inversion of the likelihood ratio, which adds computing cost. Utilizing two stages reduces computing time over POSIRP-LR, while also obtaining tighter confidence regions.

REFERENCES

Fan, J., and Gijbels, I. (1996), *Local polynomial modelling and its applications*, Vol. 66 of *Monographs on Statistics and Applied Probability*, London: Chapman & Hall. 3

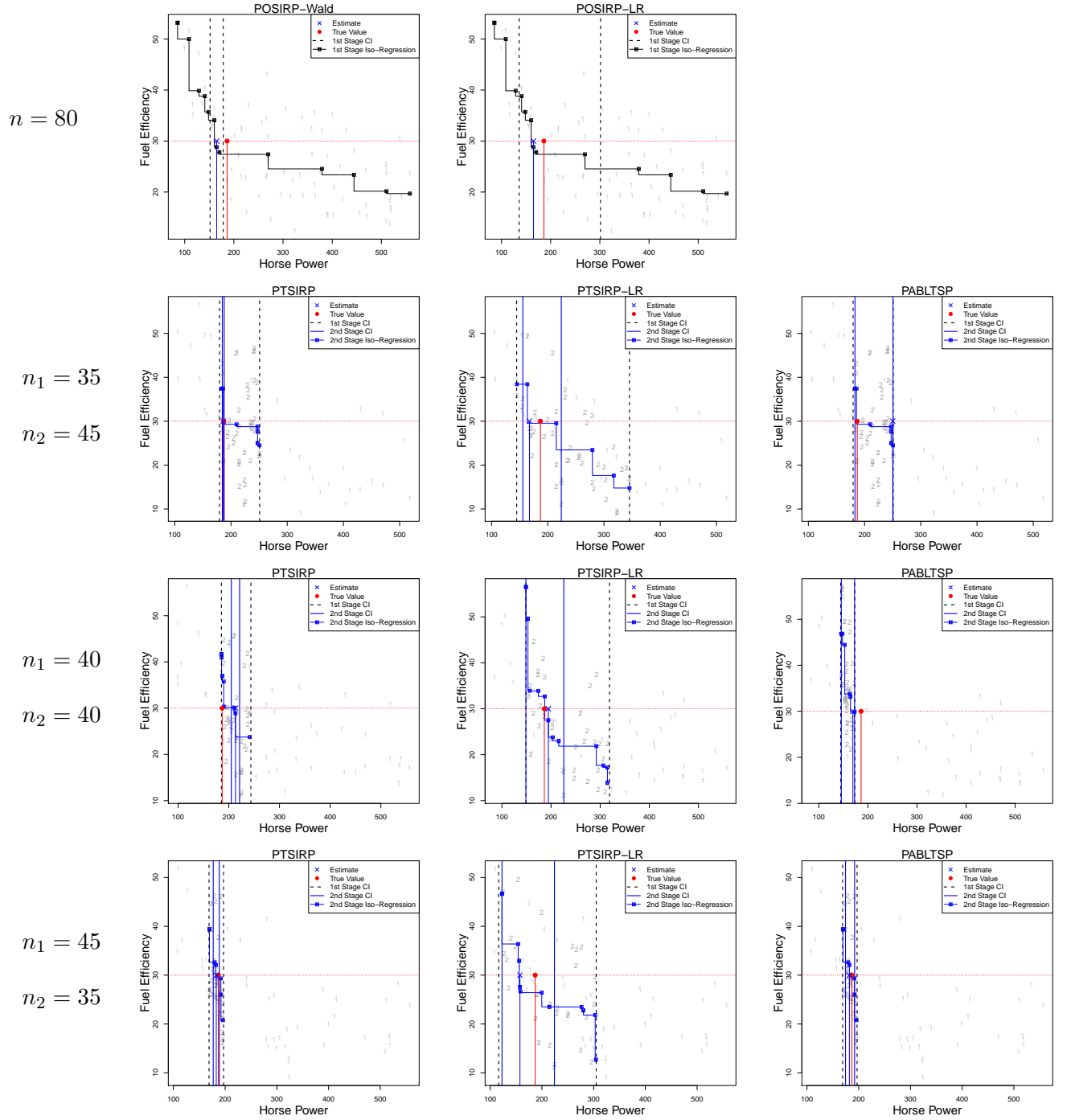


Figure 3: Plots for the data analysis with different budget specifications.

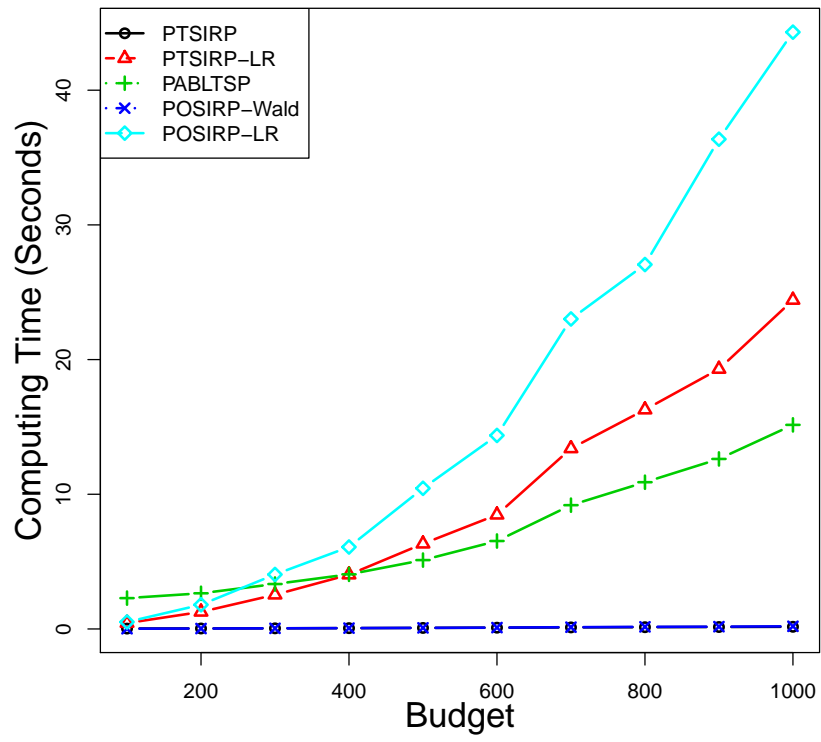


Figure 4: Average computing times with different budgets for the isotonic sine example.